University of Exeter coursework header sheet

ECMM102 Group Project (Meng) (A, TRM1+2 2016/7)

025218

1027442

630024481

Coursework: Individual contribution to the group achievement

Submission Deadline: Thu 11th May 2017 12:00

Personal tutor: Dr Mustafa Aziz

Marker name:	G_Tabor
Word count:	9542

I2 Report

Experimental Investigation of Flow Inside Draft Tubes with Varied Diffuser Geometry

James Angus

2017

4th year MEng Group Project

I certify that all material in this thesis that is not my own work has been identified and that no material has been included for which a degree has previously been conferred on me.

Signed..

College of Engineering, Mathematics, and Physical Sciences
University of Exeter

I2 Report

ECMM102

Title: Experimental Investigation of Flow inside Draft Tube with Varied Diffuser Geometry

Word count: 9542
Number of pages: 32

Date of submission: Thursday, 11 May 2017

Student Name: James Angus
Programme: MEng
Student number: 630024481
Candidate number: 025218

Supervisor: Prof Gavin Tabor

Abstract

Draft tubes are conduits connected between the exit of a hydraulic turbine and the tail race which are designed to convert wasted kinetic energy of the flow into useful static pressure to improve turbine performance. Draft tube design is a critical factor for hydropower plants which rely on low head water resources to generate electricity, with as much as half of the energy losses occurring with the draft tube itself.

This project forms a part of a greater project aiming to create an optimiser which can produce optimal draft tube diffuser geometry using machine learning and CFD simulations. The objective of this project was to provide experimental data to validate the simulations by measuring the properties of the flow within 1:220 draft tube scale models. The draft tube design chosen as the basis of optimisation was the Hölleforsen (Turbine 99) draft tube which has been investigated extensively.

Four 3D printed scale models with different diffuser geometry were produced and tested, under non-steady state conditions. The four designs included the original Turbine 99 geometry, two developments of this design to test limits of the CFD simulation and an optimised design. The results from the tests had shown that the increase in the pressure recovery factor shown by the optimised draft tube was insignificant in contrast to the other models tested.

Keywords: 3D Printing, Hydropower, Optimisation, Diffuser

Table of contents

1. Introduction and background

1.1. Background

For hydraulic turbines, the kinetic energy of the flow leaving the turbine represents the loss of energy which could potentially be used to generate electricity. To reduce this loss a diffuser, known as a draft tube, is connected to the turbine exit to reduce the velocity of discharged water and increase the available static head across the turbine. Leading to improved energy extraction from water flow and therefore greater electricity generation.

The design of the draft tube is a crucial factor in the performance of hydropower plants which utilise low head water resources, with up to half of the energy losses for these plants occurring within the draft tube itself [1]. The influence of the draft tube on the efficiency of power generation can have significant impacts on the profits made by powerplants considering that draft tubes can be installed and expected to last over decades. However, any designs are also conflicted with the substantial civil costs of installing them in the first place. Thus, designs consider this aspect against the anticipated money generated from the improvement of the design.

The optimisation of draft tube design is focused on maximising the pressure recovery between the draft tube inlet and outlet, thereby increasing the amount of extractable pressure energy. Factors that influence this and the performance of turbines are head loss, cavitation and flow separation which are dependent on draft tube geometry and make its design a complex task.

The Hölleforsen (Turbine 99) draft tube was chosen as the object of optimisation, having been used as a test case for numerous studies trying to understand simulate the flow inside, it provided the investigation with a basis from which the CFD simulations could be built on. The draft tube was also chosen based on its potential for improvement because of the square diffuser geometry it possessed and lent itself to a basic two dimensional profile optimisation that could be extruded into 3D.

1.2. Project Aim

The aim of this project was to develop an optimiser which could provide an optimal draft tube design, specifically for turbines with low head application, by employing machine learning in conjunction with CFD simulations. Experimental work performed as part of the project was used to validate the CFD simulations, by providing flow data from tests performed on a scale models of the simulated draft tubes.

1.3. Objectives and Deliverables

The following are the objectives and deliverables for this experimental part of the overall project [2].

Objectives

I. Design an experiment to measure the pressure drop between select cross-sections including the inlet and outlet, along with flow rate and velocity profiles.
II. Explore and produce physical versions of the models used in CFD simulations which can withstand stresses during experimentation and enable flow measurements.
III. Measure and provide an estimate for the model surface roughness.

Deliverables

I. Four scale models which can be used for experimentation.
II. An experimental setup which can be used to measure pressure drop between select cross-sections of the model, including inlet and outlet, along with inlet flow rate and velocity profile at the outlet.
III. A range of the surface roughness values for the scale models.
IV. Pressure drop and pressure recovery values between the inlet and outlet for all the scale models.
V. Outlet velocity profile for all scale models

2. Literature review

2.1. Turbine 99 Workshops

Extensive investigations had been made into the simulation of flow through the draft tube of the Kaplan turbine used at the Hölleforsen hydropower plant, Sweden, as part of the “Turbine-99” workshops [3, 4], which took place on three occasions: 1999, 2001 and 2005. The intensions of these workshops were to improve upon the understanding of the flow inside draft tubes as well as the capability to simulate it and identify improvements to the design.

The draft tube at the Hölleforsen power plant, Figure 1, (also referred to as the Turbine 99 draft tube) is an old design, built in 1949 [5] It was stated to need refurbishment and had been chosen to be the subject of investigation since it was the most relevant: technically and problem-wise for the industry [1]. Further reasons mentioned included the ability for it to be easily optimised due to its sharp cross-sections and the fact it is part of a Kaplan turbine in which the draft tube can have a considerable influence on its performance.

Simulations using Computational Fluid Dynamics (CFD) were performed for the workshops and accompanied by experimental studies, performed on a test rig which replicated the Hölleforsen power plant on a 1:11 scale, and have been summarised by a thesis [1]. The test rig recreated the conditions the draft tube would experience and operated at two operating points on the propeller curve, top (T) and right leg (R), conducted at 60% load. The tests performed under these operating points were at a temperature of 15°C, with flow rates of 0.522 and 0.542 m^3/s for points T and R respectively [3]. The amount of swirl produced from the flow, which varied depending on the operating conditions, was stated to affect the performance of the draft tube.

Measurements of velocity and pressure were made at select cross-sections of the scale model, see Figure 1. Velocity was measured using Laser Doppler Velocimetry, LDV, (C.S. Ia, II & III), pressure was measured using a three-hole Pitot tube at the inlet (C.S. Ia) and pressure tappings at the outlet (C.S. IVa, IVb). which were used to calculate flow properties to validate CFD simulations, this included the pressure recovery factor between the inlet and outlet of the model.

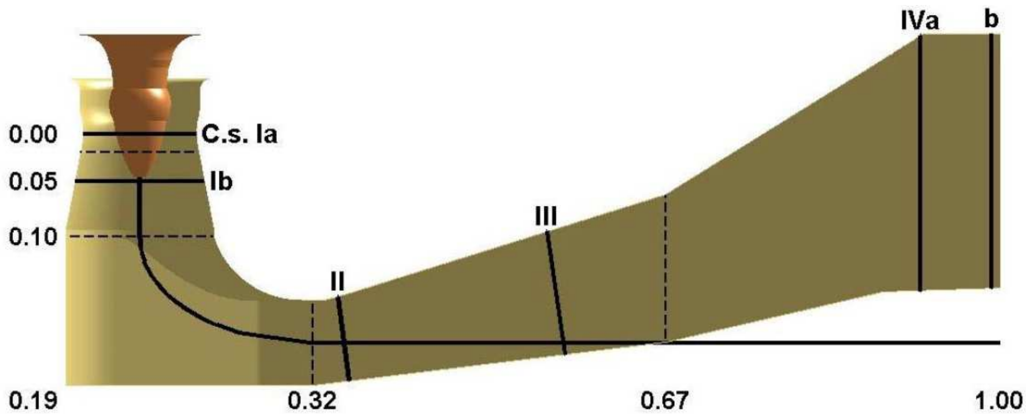

Figure 1, Cross-sections at which measurements were made on the Turbine 99 workshop 1:11 scale model draft tube. Runner cone shown in orange.

One of the findings from the study had shown that most of the pressure recovery (over 80%) occurred in the cone immediately before the elbow. Discrepancies between computed and experiment values for inlet wall pressure has also been found. The computational grid of 700k elements used at the inlet (C.S. Ia) was suspected not to be fine enough to resolve the changes in pressure as the wall is approached since experimental values of wall pressure showed a trend of increasing whilst the computational results showed a decline.

3. Theoretical Background, Experimental Work and Design

3.1. Draft Tube Theory

A draft tube is conduit which is attached between the exit of the runner in a hydropower turbine and the tail race. The shape of the draft tube diverges in the direction of the flow causing a decrease in velocity (v) and an increase in static pressure (P), resulting in a negative pressure gradient opposite to the flow. The result of this a decrease in the pressure at the turbine exit which overall increases the static pressure across the turbine. This is explained by equation 1, derived using Bernoulli's equation, and equation 2 with the subscript of the variables referring to points in the hydraulic turbine – draft tube system as shown in Figure 2. With difference in height between points 2 and 3 (H), Head loss (h_f), density of water (ρ) and acceleration due to gravity (g).

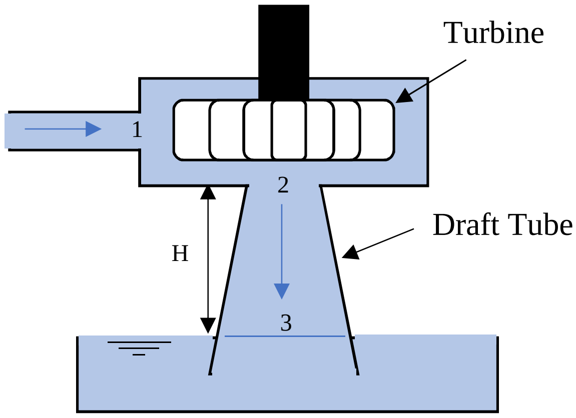

Figure 2, Diagram of a basic hydraulic turbine - draft tube system

$$P_2 = P_3 - \left[\frac{1}{2g}({v_2}^2 - {v_3}^2) + H - h_f\right]\rho g \quad (1)$$

$$P_{turbine} = P_1 - P_2 \quad (2)$$

Pressure at point 3 is atmospheric, and all the variables in equation 1 are also constant due to the fixed geometry of the draft tube, apart from flow velocity and head loss, which influences the pressure at point 2. To maximise pressure across the turbine, the pressure at point 2 needs to be minimised. For a set flow rate this is determined by the draft tube geometry.

3.2. Requested Experimental Data

Specific experimental data was requested to provide a metric from which the draft tube and CFD simulation performance could be measured and to investigate assumptions made in the CFD simulations.

N.B: Due to delays to the project because only pressure recovery factors for the models and surface roughness estimates were provided.

Pressure recovery factor

The pressure recovery factor (Cp) is a measure of diffuser performance at converting kinetic energy into pressure and thus a measure of the draft tubes ability to increase pressure across the turbine.

$$C_p = \frac{P_2 - P_1}{\frac{1}{2}\rho v_1^2} \tag{3}$$

$$C_p = \frac{g(h_2 - h_1)}{\frac{1}{2} v_1^2} \tag{4}$$

The pressure recovery factor between inlet and the selected cross-section was determined by measuring the pressure drop between these cross-sections and the velocity of the flow and then implementing these values in equation 3, with subscripts 1 and 2 referring to the inlet and specific cross sections respectively. This equation was simplified to equation 4 for the manometer readings (h), with h_2 referring to the average reading for the specific cross section measured. This value was not only compared with data from simulations but with other models that were tested to assess any improvement.

Velocity profiles

Velocity profile of the outlet was intended to be measured to investigate the symmetry of flow and thus understand the appropriateness of simulating half of the draft tube. This also provide another set of data for comparison with simulated results.

Model Surface Roughness

The surface roughness of the scale models was estimated to provide data of the scale models which may impact the simulation accuracy which assumed perfect smoothness.

3.3. Experiment Design

The experiments were designed to provide the CFD team with the requested experimental data by performing tests on a 1:220 3D printed scale model of the Turbine 99 draft tube being simulated and selected developments of its design. This included two designs that tested the ability of the CFD simulations to represent unique geometry and a design produced by the optimiser. With reference to Figure 1, the scale model produced for experimentation excluded the runner cone geometry and only incorporated the geometry between C.S. Ia to C.S. IVb, this was done to simplify the geometry being optimised and the construction of the model. The experiment provided limits to the conditions under which simulations could be run, therefore the experiment was also designed to replicate the real conditions the draft tube would experience as best as possible to improve the usefulness of the project to industrial applications. The tests performed collected real time flow rate data which was collated and displayed by a custom-made data collection system [6]. This system was also designed to measure and collect flow velocity and pressure data however neither property was measured due to time limitations and issues with recording data respectively.

Model draft tube CAD files, design drawings, raw experimental data, 3D printing files and calculations can be found through the link:

https://drive.google.com/drive/folders/0B-yRJvnMwcgbRklGSGsxWllWaXM

3.3.1. Measuring Flow Properties

An experimental setup, Figure 13 and Figure 11, was designed to measure: pressure, flow rate and flow velocity at specific cross-sections of the scale model. The tests were performed using the Armfield F1-10 Hydraulics Bench which pumped water through the model and provided a channel for submerging the model as well. The flow varied from the conditions as created in previous experiments on this draft tube design [1] which had a turbine at the inlet and higher flow rates and Reynolds numbers (Table 1) and therefore could not be directly compared with results from these experiments. The temperature of the water during experimentation was recorded using a digital thermometer (ATP Thermometer DT-613) to provide accurate values of density and dynamic viscosity to use in calculations of Reynolds numbers and pressure recovery factor. During experimentation, the mean temperature value was found to be 23.1°C, the sources for density and dynamic viscosity values at this temperature which were used in calculations can be found in [7] and [8] respectively.

Measuring Flow rate

Flow rate was measured before the inlet to the experimental model using a turbine flow meter. Two methods were used to measure the display the data from the flow meter which were via an LCD screen on the data collection system and via a digital counter, the details of which are elaborated elsewhere [6]. The latter device was used when performing tests on models 1 and 2, this was because at the time the data collection system was still unable to function and thus was used as a replacement method of measuring flow rate.

The flow meter had an accuracy of 3% therefore the flow rate was set to be within 3% of the desired value. Once the flow rate remained within this bound for ten readings the experiment was started, data from that point onwards was used in calculations, until experimental measurements stopped.

Producing Flow Within the Model

Consistent flow had to be produced through the draft tube model which enabled adequate time to take measurements of pressure, flow rate and flow velocity. The differences in the Reynold numbers at the outlet of the 1:11 model under the two realistic operational modes previously tested (T & R) at 15°C [3] and the 1:220 model tested at a mean temperature of 23.1°C is shown in Table 1. The equation used to calculate the Reynolds number (Re) is shown in equation 5, using the wetted perimeter (p_w), flow rate (Q) and values of density and dynamic viscosity (μ).

$$\mathrm{Re} = \frac{4\rho Q}{\mu p_w} \tag{5}$$

Scale	Operational mode	Flow rate (m^3/s)	Wetted Perimeter of Model Outlet (m)	Reynolds Number
1:11	T	5.22E-01	4.13	443903
1:11	R	5.42E-01	4.13	460910
1:220	n/a	5.00E-04	2.06E-01	10365

Table 1, Flow rate, outlet wetted perimeter and Reynold numbers for the 1:11 turbine 99 draft under the two operational modes T & R and the 1:220 model used in the experiment.

The flow rate for the experiment was maximised to increase the Reynolds number of the scaled model as close as possible to realistic operating values, seen in Table 1. This was constrained by the flow rate meter operating limits, which limited the flow rate to a maximum of 0.5L/s [9].

The maximum flow rate that could be produced through the experimental setup was approximated by comparing the total expected head loss from the setup between the outlet of the hydraulics bench pump and the outlet of the draft tube model against the pump curve [10]. The hydraulics bench was first tested at its maximum flow rate with just the tubing section of the experimental setup connected to provide an estimate of the maximum head loss for this part of the experimental setup. The remaining sources of head loss of the experimental setup, excluding the hydraulics bench, were calculated using the Darcy-Weisbach equations. With the head loss from the model estimated by simplifying the model to a square elbow pipe bend and a conical diffuser with closely resembling geometry. Plotting the total estimated head loss against the pump curve of the hydraulics bench, a maximum possible flow rate of approximately 0.65 L/s and allowance for a head drop of 1.5m H_2O was found. Therefore a flow rate of 0.5 L/s through the setup was possible. The flow rate was adjusted to reach this value using the throttling value on the side of the hydraulics bench.

Measuring Pressure

Pressure tappings were used to collect pressure data at select cross-sections (CS) of the models, shown in Figure 3. The inlet (CS1) had one tapping and the cross-sections between the inlet and outlet (CS2 – CS4) had tappings positioned at the midpoint of each face of the model, with CS2 only having three tappings (sides and bottom face), shown in Figure 5. The positions of the tappings were maintained for all models except for the developed diffuser designs which just had no tappings on the altered side. The outlet (CS5) had eleven tappings, based on and scaled to the outlet tapping arrangement used in the Turbine 99 workshop experiment [3].

Cross-sections CS2 – CS4 had been chosen as areas of interest on the model. Pressure at CS2 and CS3 were chosen to be measured to understand the change in pressure recovery just after the elbow and to provide an indication of the losses associated with the flange. CS4 was chosen to provide another set of data for how the pressure recovery factor changes as flow passes through the model. The measured results from the tappings at these cross-sections were averaged to provide a value of pressure over the area.

The tappings were designed to be used in conjunction with two measuring instruments, manometer board and pressure sensors, to obtain values of pressure drop between two select cross-sections. The manometer board consisted of 12 channels which were connected to two sets of tappings at a time: inlet and outlet tappings, and inlet and the tappings at CS2-CS4. Five pressure sensors were intended to be used which would have measured the pressure between the inlet and a set of four other tappings sequentially. The tappings which were not being used were capped using a short piece of tubing with a white section of plastic rod inserted at one end, as can be seen in Figure 6. The tubes connected the model to these instruments and were made to be minimal in length as practical for the experiment to reduce the settling time of the pressure response to be within a range close to the true pressure [11]. This was important as this increased the chances the true pressure value would be recorded by the data collection system which had a fixed sample rate.

The diameter of the tappings were fixed at 2mm, which was four times the minimum hole diameter that was achievable via the 3D printer, to help ensure the hole could be produced successfully. This size of tapping had also been deemed a practical size to reduce slow response from the flow [12].

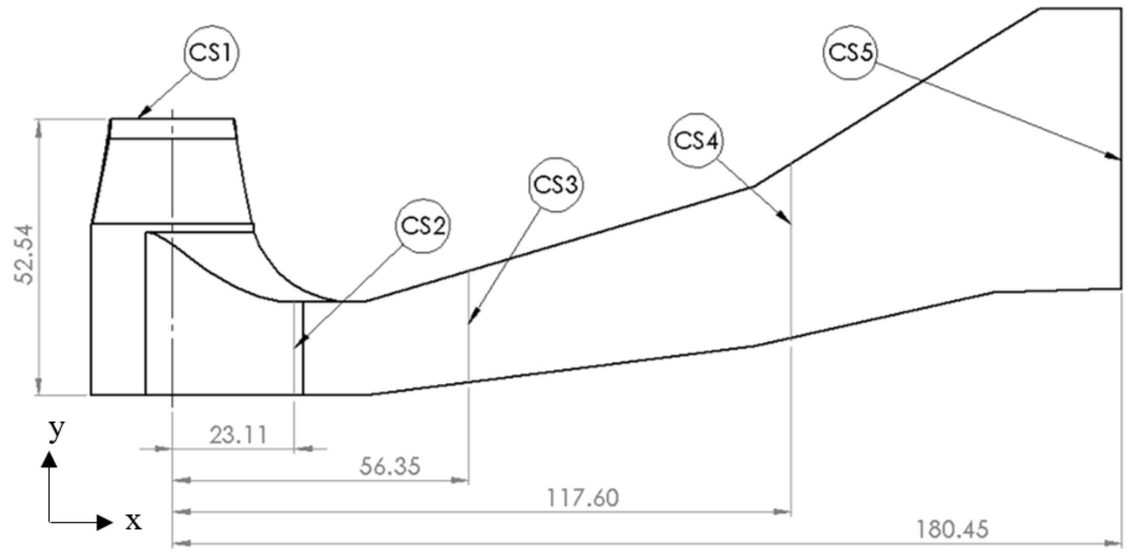

Figure 3, Cross-sections (CS) at which the pressure tappings were located on the experimental model, shown on the 1:220 scale model of the actual draft tube, dimensions in millimetres.

Measuring Velocity Profile

The velocity profile was designed to be measured using a flow meter probe (Nixon Flowmeter 403), positioned to collect velocity data at specific points which would cover the area of the outlet. The probe was connected to an indicating instrument (Nixon Streamflo 430), which collected data in the form of frequency of the probe propeller revolutions. This frequency data was transferred to the data collection system and would then be converted to velocity via a conversion chart associated with the probe. The points the probes were positioned in were dictated by the area over which the probe measured velocity, the grid showing the points at which the probe head would have been located is shown in Figure 4.

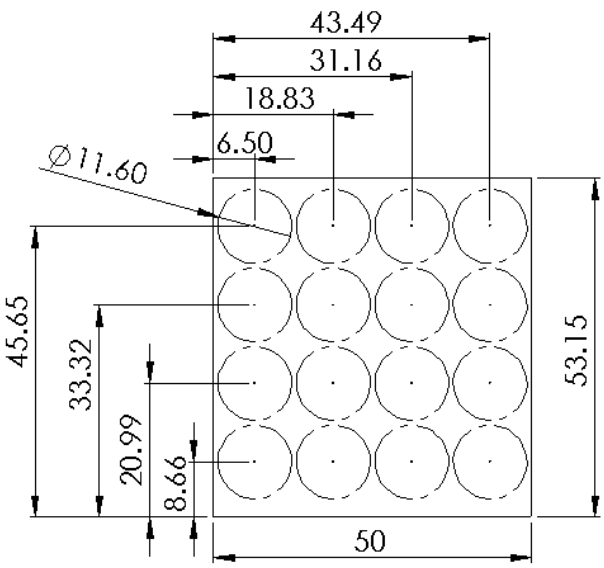

Figure 4, Positions for axis of flow meter probe at the 1:220 scaled model outlet, viewed straight on, solid lines and dashed lines representing outlet area and area over which velocity is measured respectively, dimensions in millimetres.

3.3.2. Draft Tube Model Design and Manufacture

The models were produced using the Formlabs 2 stereolithographic 3D printer with the Formlabs standard clear resin (V2). The alternative viable manufacture method was CNC which had been considered as an option for this project, although in comparison, 3D printing had provided benefits over this method. Using 3D printing had meant that no further manufacturing had to be done, reducing the effort of producing the models to simply finishing surfaces and removing blockages from tappings. Whereas CNC produced parts of the model would have required more time and effort to assemble and make experiment worthy. It had been noted that 3D printing was a more expensive option although for the project only few models had the capability to be made and tested thus it was possible with the budget for the project to use this method which was more time effective. This was important since it meant there was greater potential to experiment on more designs and provide more validation data against solutions found from the optimiser, aiding in understanding of its performance.

The scale model used for experimentation was adapted from original draft tube design, shown in Figure 3, to make it experiment worthy, the changes are shown in Figure 5. The experiment scale model was made to be as large as possible relative to the designed experimental setup including being able to be submerged with the upper channel of the hydraulics bench. This was done since it meant that the tapping diameter in relation to the perimeter of the associated cross-section could be as large as feasible reducing the disturbance on the flow caused by tappings, leading to a more accurate pressure reading. The limited print space and budget constrained the scale of the model to a maximum of 1:220 of the real world turbine 99 draft tube geometry to be able to produce the set minimum of three models for testing. The models were made from two sections (elbow and diffuser) which were individually printed and then attached, the two halves assembled for model 1 is shown in Figure 5. This had enabled reduced printing since it meant that only the diffuser section had to be printed and exchanged to produce new models for testing. The geometry of the outlet was chosen to be fixed since this resembled a realistic constraint in terms of construction.

The 3D printed material can be considered as isotropic [13], this was considered when designing the scale model for experimentation.

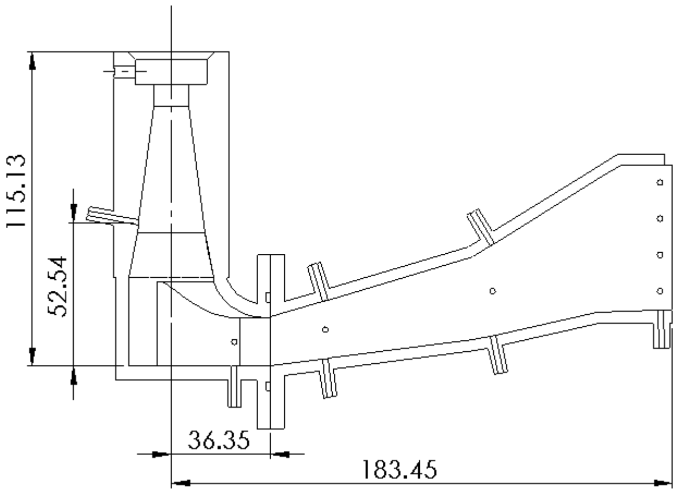

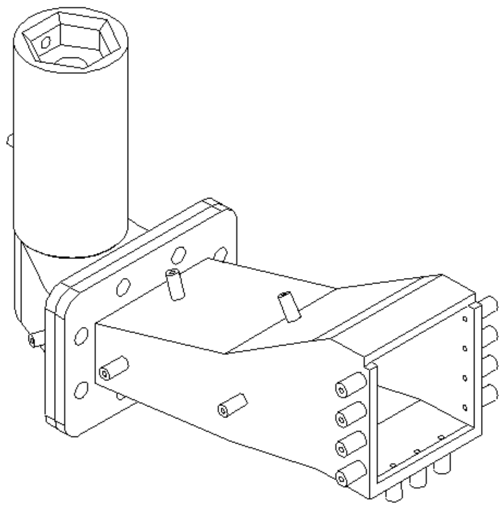

Figure 5,CAD drawings of model 1 elbow and diffuser section assembled: side view of half of model 1 (left), Isometric view of whole model 1 (right), dimensions in millimetres.

Flange Design

A flange connected the two halves of the model together with a water tight seal. The Flange design was based on an existing full face grooved flange design for a wave guide with rectangular duct geometry (catalogued as CPR 187 DES-10) [14, p. 60]. This was chosen since this closely resembled the dimensions of the rectangular cross-section at which the model was divided and thus provided an appropriate bolt loading when assembled. This form of connection was chosen since it incorporated an O-ring which meant the flange does not require high bolt stress to achieve a seal [15]. The groove of the original flange design was adapted to fit a 2.5mm O-ring using dimensions from an existing groove design (O-Ring Parker Size 102) [15, p. 98]. M6 bolts, nuts and washers were used to fasten the two halves together with two M6 studs manufactured to be able to fit into two flange holes on the top side of the model as shown in Figure 6.

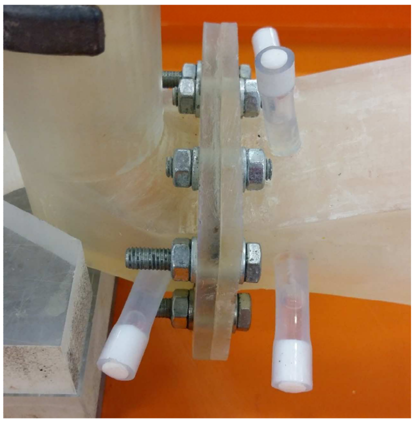

Figure 6,Close up of flange when model is assembled

Pre-3D print setup

Support structures are generated by the Formlabs software to support the model during the printing process as shown in Figure 7. Within the available print space, the model was orientated at specific angles which were recommended to achieve a successful print [16]. For printing flat surfaces, the minimal angles suggested were chosen to maximise the available print space for the diffuser geometry. The potential print space of the model was dictated by these constraints. The layer height for the print was specified as 100 microns since there was available mechanical data for the resin used with this print setting [17], this data was used when designing the model to withstand certain stresses.

Post print processing

The model was extracted from the printer and cleaned using the procedures set out by Formlabs [18]. The model was then cured under UV light using the Mechitronicore BB Cure system under the conditions of 405ηm UV exposure at 40°C for 60 minutes. The same mechanical data for the resin, as mentioned for the layer height of 100 microns, had also been treated under these conditions. Once cured the supports were removed using pliers. The models were then finished using two grades of wet and dry paper (P120 then P1000) on the inner and outer surfaces of the model to remove any support marks left over after most the scaffolding had been removed. This was also done to make the inner surfaces as smooth as achievable to come close to matching CFD conditions of perfect smoothness.

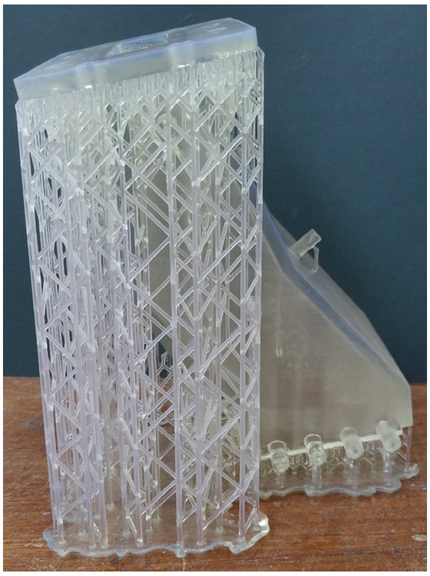

Figure 7, Diffuser section of model 4 post cure with support structure still attached

Wall Thickness

The model was designed to withstand the force applied from the maximum water flow (0.5 L/s) when submerged. It was assumed that the point at which the momentum change, therefore the point at which maximum force would be applied, was at the sharp heel of the model. Therefore, the section of the model heel at which the largest deflection was expected, was used to provide an overestimate of the required thickness for the model, Figure 8. This section was chosen since it had the greatest width within the elbow. The maximum force was calculated, based on the momentum change, with the control volume being between the inlet and outlet of the model, CS1 and CS5 from Figure 3 respectively. The axis also shown in Figure 3 was used as reference in the calculations.

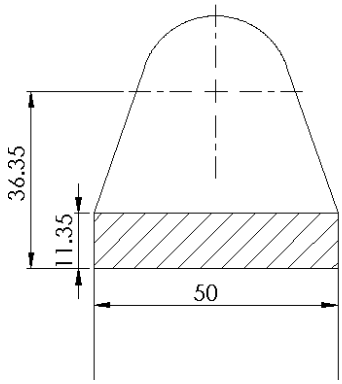

Figure 8, bottom side view of heel, hatched area showing section used to overestimate deflection, dimensions in millimeters

To obtain the force applied to the model, the value of inlet pressure was estimated using Bernoulli’s equation and the pressure at the outlet. The hydrostatic force at the outlet, when the model would be submerged, was determined so the outlet pressure could then be calculated, this was done using the pressure prism method. Considering the outlet to have zero thickness for calculations and considering an arbitrary depth (H_d) to the lower edge of the outlet relative to the water surface, the hydrostatic force (F) was calculated using the height of the outlet (H_{out}), Figure 4, using equation 6. The pressure of the outlet was found by dividing this force by the area of the outlet.

$$F_{out} = \frac{1}{2}\rho g H_d - \frac{1}{2}\rho g (H_d - H_{out}) = \frac{1}{2}\rho g (H_{out}) \tag{6}$$

Applying Bernoulli's equation between the inlet and outlet of the control volume, excluding head losses, the pressure at the inlet was found using equation 7. The difference in height of the two points (Δz) was relative to the centres of the inlet and outlet.

$$P_{in} = P_{out} + \frac{\rho}{2}({v_{out}}^2 - {v_{in}}^2) + \rho g(\Delta z) \tag{7}$$

The force applied to the heel (F_h) was resolved in y axis and calculated using equation 8, with the pressure forces (F) and mass flow rate (ṁ). The force in the x axis direction was ignored since enough support was provided by the elbow stand in this direction for there to expect no to very minimum deflection.

$$F_{hy} = \dot{m}v_{outy} - \dot{m}v_{iny} - F_{outy} - F_{iny} = -\dot{m}v_{iny} - F_{iny} \tag{8}$$

The velocity and pressure force from the inlet acted downward, and thus were negative. There was no component of force or velocity in the y-axis from the outlet, therefore those terms were removed from the equation.

With this resolved force, the deflection (d) at the centre of the specified section, Figure 8, was calculated using equation 9 [19] for a range of thicknesses to identify the most appropriate. The variables used were, the length of the section (L) the first moment of area (I) Young's modulus of the 3D printed material (E) [17].

$$d = \frac{F_{hy}L^3}{48EI} \tag{9}$$

A thickness of 4mm and 5mm provided a deflection of 1.33mm and 0.68 under the overestimated force respectively. A thickness of 5mm was used for the elbow section since it provided a deflection lower than 1mm which was deemed acceptable in an area suspected to receive most of the impact from the water entering the model.

Since the calculations are based on the force at the heel of the model, which were anticipated to be much higher than the rest of the model, the thickness of 4mm for diffuser was thought as acceptable.

Tapping Connection Design

The tapping connections were designed to provide a tight connection between tubing and the tappings of the model. The connections are the hollow cylindrical features on the outside of the model which were designed to fit tubing connected to either the manometer board or pressure sensors, these can be seen in Figure 5. The tubing had a fixed inner diameter of 5mm, therefore the connectors were designed around this dimension. The fit between the tubing and connector was designed to be a locational clearance fit (5H7/h6 tolerance, ISO fit) to enable a snug fit that could still be disassembled. The length of the tapping connectors were specified to be 10mm since this provided space to fit cable ties around the circumference of the connector without slipping. Cable ties use was featured into the design in case the fit of the tubing was too loose. This length also provided adequate grip for the tubing to be fitted.

Model Inlet Design

The inlet of the scale model was designed to be able to connect to the tubing from the pump outlet of the hydraulics bench to CS1 of the draft tube. To connect to the tubing, a hose tail was used which screwed into a nut glued into a recess at the model inlet, shown in Figure 9. A dowel pin was horizontally inserted at the top of the model into the nut to strengthen the attachment against any force from the thrust of the water entering the model, this can also be seen in Figure 9. A converging section of pipe was incorporated into the model inlet design which created a gradual change in cross section from CS1 to the hose tail diameter to minimise head loss, this can be seen in Figure 5.

Figure 9, View of model inlet and elbow section with model placed on stands

Draft tube model stands

Two stands were manufactured to support and help position the elbow and outlet section of the model. To provide enough space for the tubing to connect to the tappings on the lowest point of the model a minimum clearance of 40mm was given between the base of the hydraulics bench channel and the model, this factored in the capability for the model to still be submerged. This clearance was given as a constraint for the design of the stands. The elbow stand consisted of two layers of acrylic and a bottom (base) layer of aluminium to which bolts were screwed to hold the top two layers in place, the top most had a notch in which the heel of the elbow could sit as shown in Figure 9. The stand at the elbow was weighted with a plate of aluminium to help prevent it from sliding during experimentation since it was expected that thrust would be generated counter to the flow at the outlet. The outlet stand was made from clear acrylic sections glued together, this is shown in Figure 10.

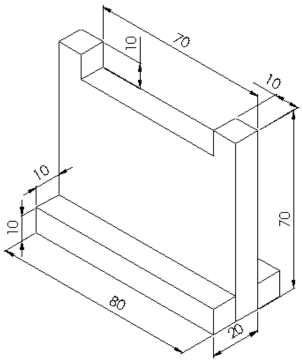

Figure 10, Isometric view of outlet stand CAD drawing, dimensions in millimetres.

3.3.3. Experimental Setup to Measure Flow Properties

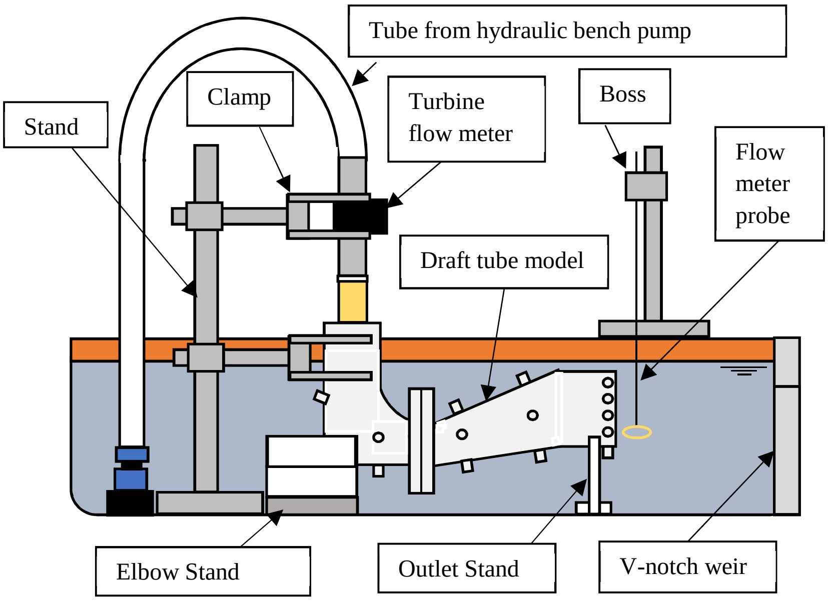

Figure 11, Diagram of experimental setup to measure flow properties within top channel of hydraulics bench, excluding clamp with ruler as seen in Figure 13.

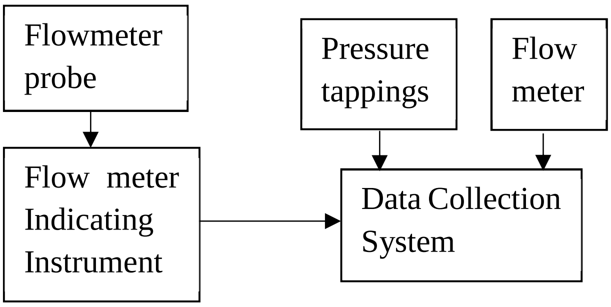

Figure 12, System diagram showing source of signals received by data collection system

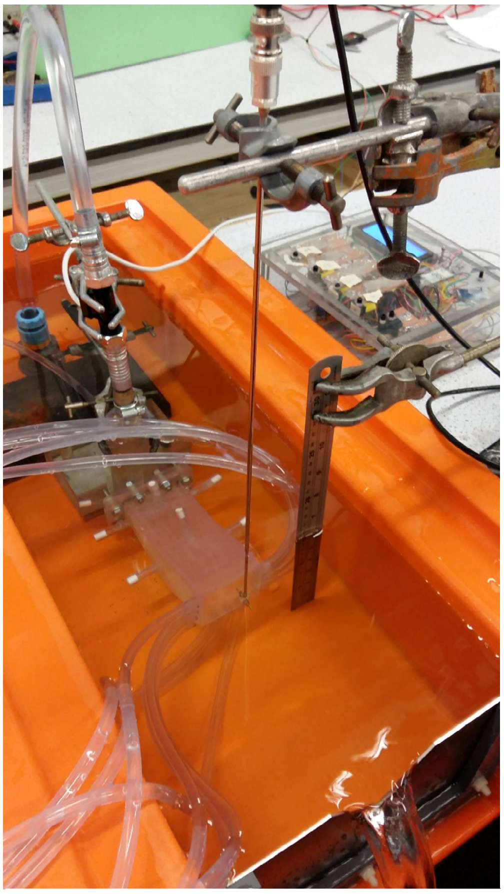

Figure 13, Experimental setup, measuring pressure drop between inlet and outlet, with tappings connected to manometer board.

The top channel of the hydraulics bench was fitted with a v-notch weir attachment to retain water so the model could be submerged and still allow water flow, this can be seen in Figure 13. The clamp and stand within the channel was used to hold the model in position and hold the turbine flow meter vertical. The turbine flow meter had two hosetails connected at either end of the sensor, one end connected to the tubing from the hydraulic bench pump and the other to a small section of tubing connected to the model inlet hose tail. A clamp and stand was also used to hold the flow meter probe in place, and a ruler held vertically and perpendicular to the base to act as a horizontal reference for the positioning of the probe. The data collection system was located on a table next to the hydraulics bench, as seen in Figure 13, next to this was the flow meter indicating instrument which was connected to the probe and the data collection system.

Tubing

Two different sizes of PVC tubing were used in the setup, one larger size with an inner and outer diameter of 12 and 15mm respectively and the other being smaller with an inner and outer diameter of 5 and 8mm respectively.

3.3.4. Method for Measuring Flow Properties

Only two flow properties were measured which were flow rate and pressure drop between the inlet (CS 1) and the outlet (CS 5). Hence the other methods for measuring properties were not performed. Tests were performed for a maximum of 10 minutes to limit electricity consumption.

Setup before Testing

The stand within the hydraulic bench was placed square to the side of the channel and moved away from the weir until it was in contact with the outlet of the bench.

The selected model sections (elbow and diffuser) were connected, with care taken to tighten up the bolts on the opposite sides of the flange in sequence to avoid warping. The bolts were initially hand tightened and then tightened with two more turns using a wrench.

The model was placed in the elbow and outlet stands within the hydraulic bench channel. The model and supporting stands were then repositioned with the outlet parallel to the weir and the model centralised within the width of the channel. The model was also place as far back from the weir as possible within the channel to avoid any backflow.

The quick release hose connector was connected to the bench outlet, and the clamps connected to the stand within the channel were tightened to fix the model and turbine flow meter in place.

The stand holding the probe and ruler were positioned within the channel as shown in Figure 13. The stem of the probe was aligned vertically, which was checked using a sprit level, with the head of the probe twisted to receive flow the right direction as dictated by an arrow on the device.

Electronics were checked to make sure they were not in danger of coming in contact with water, in particular the power supply unit for the data collection system, which was located behind a screen for protection.

The throttle valve of the bench was tightened as much as possible and then opened by two turns, the bench was then turned on. The record button on the data collection system was then pressed to enable the flow rate to be displayed. The throttle valve was turned gradually to adjust to the flow rate, which was achieved by either by observing the digital counter reading or the data collection system display. Before any of the tubing was connected to the model or before any measurements were made, the bench channel was left to fill with water whilst the bench was on.


Figure 14, Measuring the height of the probe relative to the boss with a digital Vernier calliper

Measuring Pressure Drop via Manometer Board

The tubes from the manometer board, were attached to the specific tapping connectors of interest on the model when the channel was full of water. The manometer board, which was situated on an adjacent hydraulics bench, was placed flat on top the bench with the air release valve fully open and connected to a tube which lead back into the bench with the experimental setup. A piece of flat aluminium plate was placed across the front of the outlet to encourage water flow up through the tappings and into the manometer board. Once bubbles had purged from the tubes the air release valve was closed and the manometer board up-righted. The valve was then carefully turned to allow some air back into the manometer board so the levels of the water columns within the channels could be read. The readings of water levels were taken at the lowest point of the water surface. A spirit level was used as a visual aid to ensure the water level was being read horizontally. Fluctuating water levels were recorded by video for 30 seconds, with the camera held in place focused on the approximate mean of the fluctuation.

Measuring Pressure Drop using the Pressure Sensors.

Small sections of tube (500mm in length) would have been used to connect the sensors on the data collection system to the model. These tubes would have fitted to the sensors and then held vertically and filled with water from a pipette to purge the air bubbles. The plan was then to form a u-bend with the exposed ends to prevent air entering the tubes, and then place the tube end under water. The tubing would have then been attached at the chosen set of tappings.

Measuring Velocity Profile

The probe head would have been aligned with the bottom left hand corner of the model outlet to give a point at which the probe could be moved relative to. A Vernier calliper would have been used to measure the position of the probe relative to this point, using the ruler as a horizontal reference and the boss with which the probe is attached as a vertical reference, as demonstrated in Figure 14.

3.3.5. Measuring Surface Roughness

The equivalent sand grain roughness of the surfaces was estimated since this value of roughness can be implemented into CFD simulations. Hence simulations could be run which compare the effects of including the experimental model roughness to the default perfect smoothness condition used. To measure the range of values of model surface roughness, samples of the 3D printed material, subject to the same finishing process as the experimental models, were scanned using a non-contact scanning instrument (Talyscan 150). Opaque 3D printed samples had been used because the instrument had difficulty focusing on the clear sample due to its transparency. These samples had been printed using the white standard resin, a resin with the same properties of the clear resin excluding its transparency, using the same print settings (layer thickness 0.1mm) and the same curing method (405ηm UV exposure at 40°C for 60 minutes).

The samples were two flat sections which had been sanded down using two grades of wet and dry paper (P120 and P1000) in one consistent direction, until no marks which countered this direction were visible. One sample (rough) had been sanded using the coarser paper (P120) and the other (smooth) had been sanded using both grades of paper, first P120 and then P1000, this recreated the surface finish of the models.

The profile of the surfaces was approximated to a sine wave with half the period assumed to be the mean diameter of the grains of the wet and dry paper. The Nyquist frequency of this approximate sine wave was used to provide the maximum spacing at which the scanner could take samples to represent the wave. Thus, the mean grain size was used as the maximum spacing value. The grain size for the P120 grade and P1000 grade wet and dry paper was 125 and 18.3±1 μm respectively [20]. Three scans were performed on the rough and on the smooth samples, each scan with an incremental decrease in the spacing of the measurements points in the x and y direction, starting at 15 and 120μm for the smooth and rough samples respectively. The increment was a third of the maximum spacing tested. The increase in spacing was anticipated to result in convergence about a specific equivalent sand grain roughness which could be used to provide estimation of the actual roughness. The data received was a colour plot of the surface depth which was processed using TalyMap analysis software to provide results, this included levelling of the plot in case the sample surface was at an angle to the horizontal and profile extraction which provided a plot of the profile selected.

Five profile plots of the surface were extracted from the plots at five evenly space points in the y-direction, including top and bottom edge of the plot space, perpendicular to the grooves of the surface shown on the plots. The maximum and minimum amplitudes, R_{pi} and R_{vi} respectively, were obtained for each of the five profiles with respect to the mean. The difference in amplitude of the maximum and minimum amplitudes for the five plots were averaged to provide a peak-to-valley value (R_{zd}), equation 10, which can be converted to a value of equivalent sand grain roughness (ε), equation 11 [21].

$$R_{zd} = \frac{1}{5}\sum_{i=1}^{5}(R_{pi} - R_{vi}) \tag{10}$$

$$\varepsilon = 0.978R_{zd} \tag{11}$$

4. Experimental Results and Analysis of Experimental Models

4.1. 3D Printed Models

Four diffuser section models were produced, side views of the designs can be seen in Figure 15. The top model shown has the original turbine 99 draft tube diffuser geometry. The second and third models down were created to validate extreme geometry that could be produced by the optimiser to understand the limitations of accuracy. The last model design was a solution produced by the optimiser.

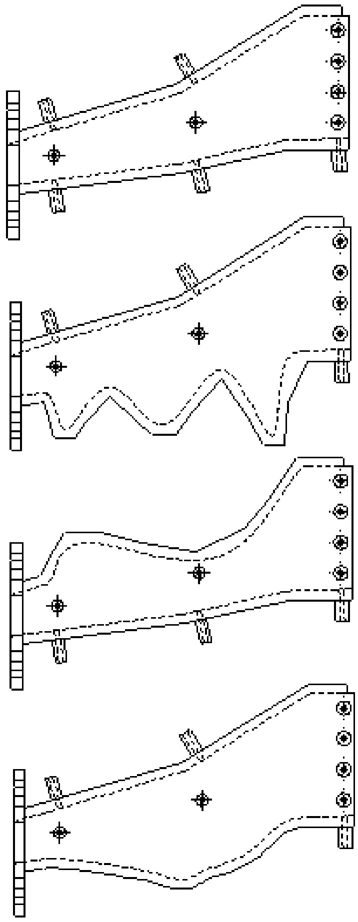

Figure 15, CAD drawing side views of the four diffuser section models produced, listed in order with top being model 1 and bottom being model 4 (optimised)

The elbow section produced, Figure 16, was re-used in all the four model tests, with no noticeable signs of wear or damage.

Printing Issues

There had been some issues identified during finishing of the model after it had been printed. Consistently the tappings had been found blocked and required drilling by hand to open them. From inspecting the blocked holes, it appeared that the angle at which the models were orientated for printing was not enough to drain the ink during the printing process.

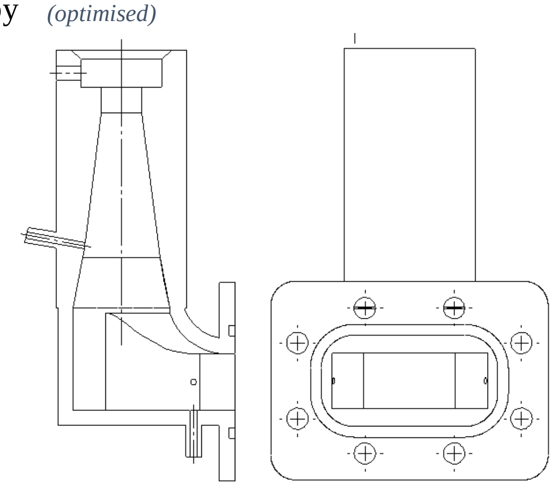

Figure 16, CAD drawing of side view, showing half of elbow section and a front view, showing the flange design

The scaffolding generated by the Formlabs software to prepare the model for printing had provided enough support for all the prints not to fail. The scaffolding is typically designed with weak points so it easy to remove, however there were a few instances where the scaffolding had fused to the tapping connecter and required sanding down to remove.

Model Finishing Issues

Model 2 in particular presented the problem of finishing models with hard to reach areas, scaffolding had been generated on the inside of the jagged geometry, and required more time to remove and finish to standard. This also presented and issue with sanding down all of the surfaces within the model, of not being able to cover all areas with exactly the same level of finish. When removing scaffolding with the pliers, it can be potentially hazardous, since small pieces fly off the model when cut. Also, when removing scaffolding via this method it had been found to chip certain weak spots of the model. When drilling tappings by hand it was also possible to chip and break off sections of the tapping connector.

4.2. Results from Flow Property Experiment

4.2.1. Inlet Flow Rate

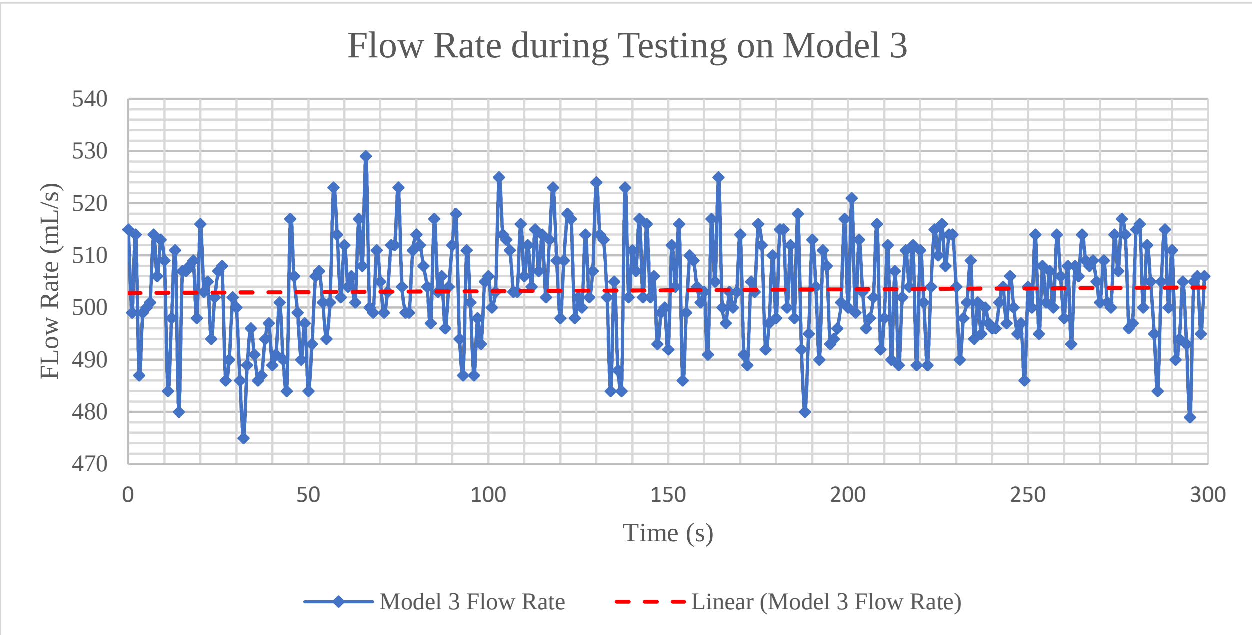

Figure 17, Flow rate over the period in which Model 3 was tested

The mean of the flow rate shown in figure 17 indicates that the values were consistently offset. The plot shows erratic flow rate changes, with the range exceeding 3% of the mean value of 504 ml/s. This may be characteristic of the sensor being used under maximum flow rate conditions. The rapid changes in flow rate also show that the flow is not under steady state conditions.

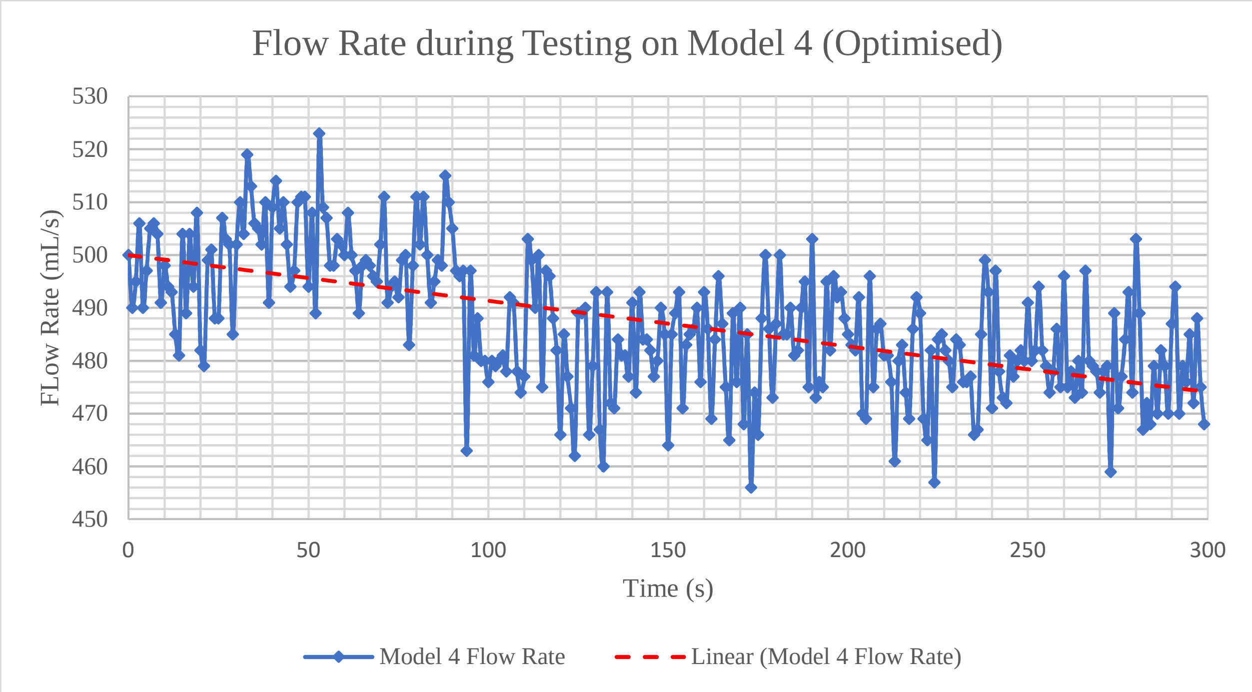

Figure 18, Flow rate over the period in which model 4 was tested

Much like Figure 17, the rapid changes in flow rate in Figure 18*Figure 1* indicated the tests performed were not under steady state conditions. The decline in the flow rate over time suggests that either the throttling value was still being adjusted or there was a fault with the hydraulics bench.

4.2.2. Pressure recovery

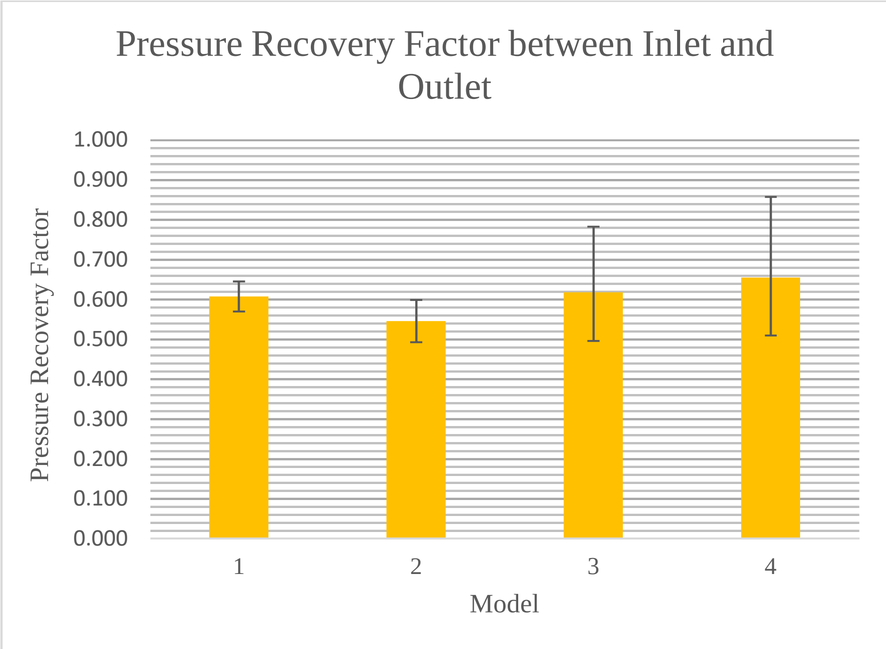

Figure 19, Final results of pressure recovery between cross-sections CS1 and CS5 for all models, models 1 and 2 used a digital counter to measure flow rate, whereas models 3 and 4 used the data collection system

	Pressure Recovery Factor between Inlet and Outlet		
Model	Mean	+	-
1	0.608	0.038	0.038
2	0.546	0.053	0.053
3	0.618	0.165	0.122
4	0.655	0.203	0.145

Table 2, End results of pressure recovery between cross-sections CS1 and CS5 for all models.

		Model			
		1		2	
	Velocity Error Included?	No	Yes	No	Yes
Pressure Recovery Factor	Mean	0.608	0.608	0.546	0.546
	+	0.038	0.042	0.053	0.057
	-	0.038	0.041	0.053	0.056

Table 3, Comparison between including and excluding velocity error on the pressure recovery factor.

When measuring the pressure drop on the manometer board there appeared to be no changes in pressure between any of the eleven tappings measured at the outlet, which was the opposite to the inlet (CS 1) which consistently had fluctuating manometer readings and relied on video footage to capture them. This provided more evidence that the experiment was not under steady state conditions. The differences in error bar amplitude between the two methods of measuring flow rate can be seen in Figure 19. The data used in the end results of pressure recovery for models 1 and 2 do not include any velocity error which could increase the amplitude of the error bars. However as seen in Table 3, the contribution it makes to the error bars of pressure recovery is at most an increase in amplitude of 0.004 which is not hugely significant. The obvious difference the measurement method of flow rate makes to the error of pressure recovery factor makes any comparison between all models unreliable. Even when comparing the pressure recovery factor between models within the same set of methods used, the differences are very insignificant.

4.3. Results from Roughness Test

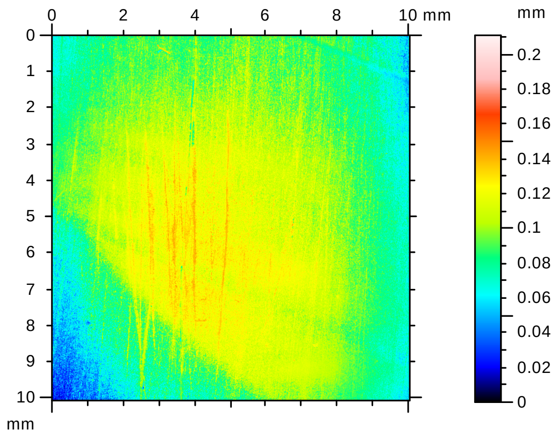

Figure 20, Levelled colour plot for depth of smooth sample with spacing of 5µm in the x and y directions.

The result obtained from the scan was a colour plot of the sample surface depths, it was obvious from these plots that the sample surfaces had been sanded at an acute angle since there was notable gradient. To rectify this levelling software from the Talyscan program was used so the mean depth of the surface was horizontal and thus the plots from the samples would be normalised. From these levelled plots, noticeable marks or indents which had not been sanded away during the sample preparation process where identified, see Figure 20, and were excluded from further post processing through using the zoom function and focusing on a section of the plot without these undesired features. The samples were found to not only have been sanded at an angle but had been sanded more intensely at the centre of the samples hence the dip which can be seen Figure 20. Both plots relating equivalent sand roughness and spacing of measurements show opposing trends, Figure 21 and Figure 22, however since the sample size is small, no definite trend can be concluded. The differences between the roughness values from higher spacing to lower spacing is approximately -4.4% for the smooth sample and 10.4% for the rough sample. The minimum spacing which could be achieved by the scanning instrument was 5µm hence to better understand the trends more data would be required, with larger and small spacings being tested for the smooth and rough sample respectively. Since convergence can not be established, to indicate a true value, for either sample, an over estimate for the range of potential values was taken. Therefore the potential equivalent sand roughness is between 44.60 and 72.96.

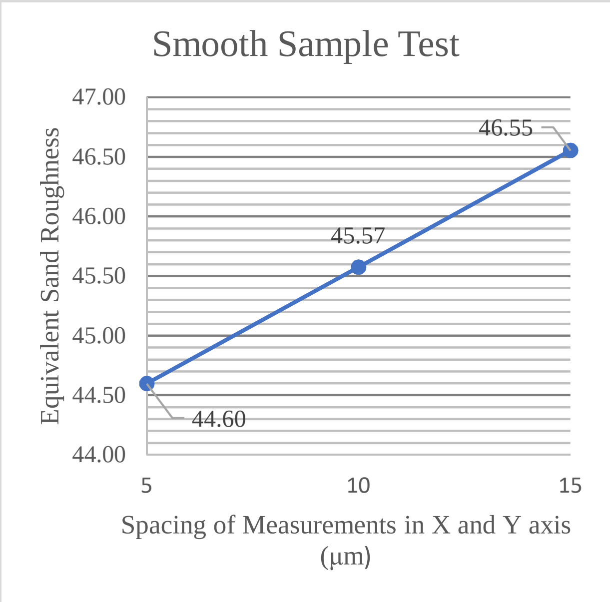

Figure 21, Results from roughness sample test

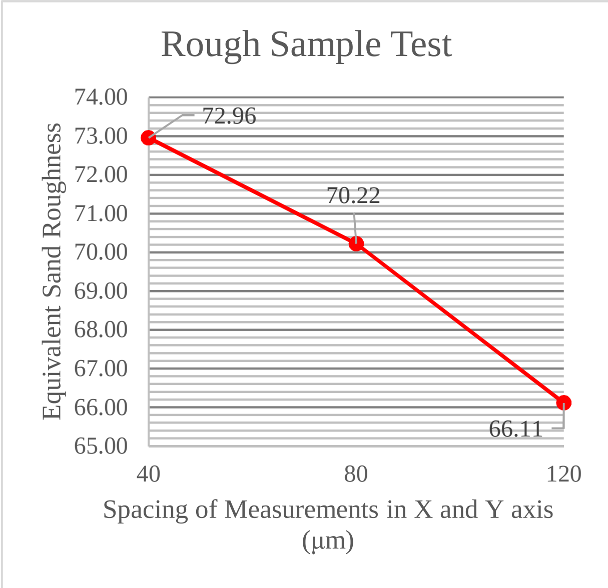

Figure 22, Results from roughness sample test

5. Discussion and conclusions

5.1. Discussion

The optimal design of the diffuser has not shown any significant improvement in terms of the pressure recovery factor which co-insides with the finding from the Turbine 99 case study that stated about 80% of the pressure recovery occurs within the cone after the exit of the turbine. The flow rate data and observations of fluctuating manometer readings at the inlet provided evidence that the flow is not in steady state.

3D printing has been shown to be a capable method of producing unique pipe geometry which can undergo experimentation and can definitely be considered for prototyping any other devices which involve water flow. It also lends its self to be a very easy material to design with since the material properties can be considered Isotopic. More care and attention needs to be provided when designing the model for printing to remove any potential sources of damage which may arise during finishing, such as scaffolding fusing with features. Also, time spent designing the model to be easy to finish by removing scaffolding from hard to reach areas could potentially be more efficient time wise than simply spending more time to finish the model.

Roughness measurements were not conclusive, with a small sample size it has been difficult to rely on any trend presented, therefore to obtain a clearer result mores samples at different spacing values need to be taken.

5.2. Conclusion

I. An experiment has been designed to measure the flow properties of scale model draft tubes which includes: pressure drop between select cross-sections including the inlet and outlet, along with flow rate and velocity profiles.

II. Four scale 1:220 models were 3D printed for experimental use, based on the actual geometry of the Turbine 99 draft tube and two developments of this design to test the performance of CFD simulations as well as an optimised design.

III. The optimised diffuser geometry has not shown significant improvement in pressure recovery factor over the other diffuser geometries tested.

5.3. Suggestions for Further Work

The cone after the turbine exit has greater potential to provide a more noticeable change in pressure recovery factors and therefore would a more worthwhile endeavour investigating for optimisation purposes.

6. Project management

Weekly group meetings were held to share and discuss progress made as well as help plan and make decisions for the future of the project and mitigate for loss of project scope. These meetings were accompanied not only by the group members but also by two PhD students and a Professor who provided advice and knowledge on the areas of CFD simulation and Optimisation methods to provide guidance to the group. Minutes of the meetings were recorded by a group member designated as secretary and chaired by a select group member as well. These roles were changed on a rotating basis. The minutes and agendas produced from and for the meetings were made to a specified format and uploaded to the group Google drive.

Deadlines for the experimental and CFD team to provide model geometry for testing were set by the dates booked for 3D printing, this was especially important since there was very limited availability of the printer.

I kept a log-book of ideas, research and work to be done which helped collect my thoughts so I could prioritise on the most important matters at the specific time of the project to enable me to work efficiently and also best manage situations were significant delays have occurred.

The other member in my experimental group had been unable to work for a long period of time due to illness which meant there were delays in the production of the circuit for measuring gauge pressure and also flow rate. I had discussed and applied for mitigation which was approved enabling use of the fluids lab and workshop in the Harrison building over the Easter period and thus meant more time was provided to perform experiments. Delays of the circuit completion had continued so other existing measuring devices (digital counter, manometer board) were used to enable at least some validation data to be provided to the CFD team so they could still have some metric to understand the accuracy of their simulations or meshes.

6.1. Health and Safety Precautions

Fluids Lab

- To prevent ingestion of water from hydraulics bench, hands were washed before leaving the fluids lab.
- Non-protected electrical equipment was placed behind a screen to prevent water from coming into contact with it.
- The floor was cleared of any water or trip hazard which could result in falling and injury.

Workshop

- Rubber gloves were worn when handling the 3D printed models during the finishing process the prevent any of the printer ink from coming into contact with my hands and thereby possible injection. Hands were also washed once gloves were removed as a second precaution.
- Safety glasses were worn to protect eyes from swarf or any other pieces which may fly off material when it is machined.
- No loose clothing was worn, to prevent being caught in machinery, such as a lathe.
- Guidance from the technicians was asked for in the event I did not know how to operate a machine safely.

6.2. Sustainability

- The model was designed for reuse and can be customised with different elbow or diffuser geometry.
- Scrap materials were used to produce the stands (elbow and outlet) for the models.

6.3. Budget

For this group project I was Treasurer. I divided the total budget (£680) of was divided into three sub-budgets; Mechanical (£265), Electronics (£215) and Emergency (£200). The Mechanical budget was focused on the materials used to produce the experimental setup, excluding the electronics, this comprised of 3D printer ink, tubing and hose tails. The Electronics budget was spent on components to produce the data collection system, which included the sensors and Ardunio Mini. The emergency budget was designed to be able to cover the costs of any expensive items becoming broken or unusable such as 3D printed models, and sensors.

7. Contribution to group functioning

The group project consisted of three teams; CFD, Optimisation and Experimental, with three group members in each excluding experimental which had two.

Within the Experimental team, I worked on the mechanical aspects of the experiment such as designing the experiment to measure fluid properties, manufacturing of model stands and design of 3D model. Whereas my other team member was focused on the electronics to produce the data logging system. Collaboration between our two disciplines was crucial to understand the implications of what we were trying to achieve and how our designs link together.

The experimental data produced from our team was given to the CFD team to verify their simulations whilst they provided our team with draft tube diffuser designs for testing. The CFD team were involved with the optimisation team as well, working together to create a method in which the optimiser could automatically run solutions through CFD simulations and receive a solution which can then be assessed by the optimiser.

8. References

[1] U. Andersson, “An Experimental Study of the Flow in a Sharp-Heel Kaplan Draft Tube,” Universitetstrykeriet, Luleå, 2009.

[2] J. Angus, P. Burns, S. Hardy, R. Gilbert, W. L. C. Ng, S. Hutchings, T. Dye and J. Gowans, “An Investigation into the Optimisation of a Draft Tube,” Exeter, 2017.

[3] F. T. Engström, H. L. Gustavsson and R. I. Karlsson, “Proceedings of Turbine-99 - Workshop 2,” in *Second ERCOFTAC Workshop on draft tube flow*, Älvkarleby, 2001.

[4] F. T. Engström, H. L. Gustavsson and M. J. Cervantes, “Proceedings of the third IAHR/ERCOFTAC Workshop on draft tube flows,” in *Third IAHR/ERCOFTAC Workshop on draft tube flows*, Luleå, 2005.

[5] D. B. Marjavaara, “CFD Driven Optimization of Hydraulic Turbine Draft Tubes using Surrogate Models,” Universitetstrykeriet, Luleå, 2006.

[6] T. Dye, “Design and Prototyping of a Custom Data Collection System for testing Scale Model Draft Tubes,” Exeter University, Exeter, 2017.

[7] W. M. Haynes, “Standard Density of Water,” in *CRC Handbook of Chemistry and Physics, 93rd Edition*, CRC Press, 2012, p. 7.

[8] ThermExcel, “Physical Characteristics of Water,” [Online]. Available: https://www.thermexcel.com/english/tables/eau_atm.htm. [Accessed 6 May 2017].

[9] RS Components, “Gems Sensors Nylon 12 Liquid Turbine Flow Meter,” RS Components, [Online]. Available: http://uk.rs-online.com/web/p/flow-sensors-switches-indicators/4468315/. [Accessed 6 May 2017].

[10] Armfield, “Fluid Mechanics F1 Complete Fluid Mechanics Laboratory - Issue 2,” [Online]. Available: http://discoverarmfield.com/en/products/view/f1/complete-fluid-mechanics-laboratory-f1-10. [Accessed 6 May 2017].

[11] I. Bajsic, J. Kurtin and T. Zagar, “The Response Time of a Pressure Measurement System with a Connnecting Tube,” *Instrumentation Science and Technology*, vol. 35, no. 4, pp. 399-409, 2007.

[12] S. Tavoularis, Measurement in Fluid Mechanics, Cambridge University Press, 2005.

[13] Formlabs, “Validating Isotropy in SLA 3D Printing,” 12 October 2016. [Online]. Available: https://formlabs.com/blog/isotropy-in-SLA-3D-printing/. [Accessed 6 May 2017].

[14] Cobham Defence Electronics Systems, “Waveguide Component Specifications and Design Handbook,” [Online]. Available: https://www.cobham.com/media/102942/cmt-waveguide-handbook-part-2.pdf. [Accessed 6 May 2017].

[15] Parker, “Parker O-Ring Handbook,” 2007. [Online]. Available: https://www.parker.com/literature/ORD%205700%20Parker_O-Ring_Handbook.pdf. [Accessed 6 May 2017].

[16] Formlabs, “Model Orientation,” Formlabs, [Online]. Available: https://support.formlabs.com/hc/en-us/articles/115000018124-Model-Orientation. [Accessed 7 May 2017].

[17] Formlabs, “FLGPCL02 MATERIAL PROPERTIES,” 19 4 2016. [Online]. Available: https://formlabs.com/media/upload/Clear-DataSheet-v2.pdf. [Accessed 6 May 2017].

[18] Formlabs, “Form 2 Basic Finishing Steps,” Formlabs, [Online]. Available: https://support.formlabs.com/hc/en-us/articles/115000024524-Form-2-Basic-Finishing-Steps. [Accessed 6 May 2017].

[19] J. M. Gere and B. J. Goodno, “Appendix G,” in *Mechanics of Materials*, Stamford, Cengage Learning, 2012, pp. 1046, 1049.

[20] FEPA, “Abrasive grains,” FEPA, [Online]. Available: https://www.fepa-abrasives.com/abrasive-products/grains. [Accessed 6 May 2017].

[21] T. Adams, C. Grant and H. Watson, “A Simple Algorithm to Relate Measured Surface Roughness to Equivalent Sand-grain Roughness,” *International Journal of Mechanical Engineering and Mechatronics*, vol. 1, no. 1, pp. 66-71, 2012.

[22] J. McNabb, C. Devals, S. A. Kyriacou, N. Murry and B. F. Mullins, “CFD Based Draft Tube Hydraulic Design Optimization,” in *IOP Conference Series: Earth and Enviromental Science*, 2014.